Structural Signatures of the Class III Lasso Peptide BI-32169 and the Branched-cyclic Topoisomers Using Trapped Ion Mobility Spectrometry – Mass Spectrometry and Tandem Mass Spectrometry

Kevin Jeanne Dit Fouque,[1] Vikash Bisram,[1] Julian D. Hegemann,[2] Séverine Zirah,[3] Sylvie Rebuffat,[3] and Francisco Fernandez-Lima *[,1,4]

[1] Department of Chemistry and Biochemistry, Florida International University, 11200 SW 8th St., AHC4-233, Miami, FL 33199, United States.

[2] Department of Chemistry, University of Illinois at Urbana-Champaign, 600 South Mathews Avenue, Urbana, IL 61801, United States.

[3] Laboratory Molecules of Communication and Adaptation of Microorganisms, National Museum of Natural History, CNRS, 57 rue Cuvier, CP-54, 75005 Paris, France.

[4] Biomolecular Sciences Institute, Florida International University, 11200 SW 8th St., AHC4-211, Miami, FL 33199, United States.

Address reprint requests to Dr. Francisco Fernandez-Lima; Address: 11200 SW 8th St., AHC4-233, Miami, FL 33199, United States; Telephone: +1 305-348-2037; E-mail: fernandf@fiu.edu

ABSTRACT

Lasso peptides are a class of bioactive ribosomally synthesized and post-translationally-modified peptides (RiPPs) characterized by a mechanically interlocked topology, where the C-terminal tail of the peptide is threaded and trapped within an N-terminal macrolactam ring. BI-32169 is a class III lasso peptide containing one disulfide bond that further stabilizes the lasso structure. In contrast to its branched-cyclic analog, BI-32169 has higher stability and is known to exert a potent inhibitory activity against the human glucagon receptor. In the present work, tandem mass spectrometry, using collision induced dissociation (CID) and electron capture dissociation (ECD), and trapped ion mobility spectrometry – mass spectrometry (TIMS-MS) experiments were carried out to evidence specific structural signatures of the two topologies. CID experiments showed similar fragmentation patterns for the two topoisomers, where a part of the C-terminal tail remains covalently linked to the macrolactam ring by the disulfide bond, which cannot clearly constitute a signature of the lasso topology. ECD experiments of BI-32169 showed an increase of hydrogen migration events in the loop region when compared to its branched-cyclic topoisomer evidencing specific structural signatures for the lasso topology. The high mobility resolving power of TIMS resulted in the identification of multiple conformations for the protonated species but did not allow the clear differentiation of the two topologies in mixture. When in complex with cesium metal ions, a reduced number of conformations led to a clear identification of the two structures. Experiments reducing and alkylating the disulfide bond of BI-32169 showed that the lasso structure is preserved and heat stable and the associated conformational changes provide new insights about the role of the disulfide bond in the inhibitory activity against the human glucagon receptor.

Keywords: BI-32169, lasso topologies, branched-cyclic peptides, collision induced dissociation, electron capture dissociation, trapped ion mobility spectrometry – mass spectrometry.

1. INTRODUCTION

Lasso peptides are a unique class of ribosomally synthesized and post-translationally modified peptides (RiPPs) exhibiting a fascinating mechanically interlocked structure [1]. All the discovered lasso peptides share an N-terminal macrolactam ring, generated by an isopeptide bond between the α-amino group and the side chain carboxyl group of a glutamate or aspartate residue, through which the C-terminal part is threaded (Figure S1). This threaded fold is predominantly stabilized by steric interactions and can also be assisted by the presence of disulfide bonds (Figure S1) [2-4]. Sterically demanding amino acid side chains (e.g. Phe, Trp or Tyr), called plugs, are needed to trap the threaded tail within the macrolactam ring and therefore stabilize the entropically disfavored lasso topology (Figure S1). The lasso peptide family is divided into four classes depending on the presence of one (class III) or two (class I) interlinked disulfide bonds and one (class IV) handcuff disulfide bond while the class II lasso peptides have no disulfide bond [5] (Figure S1). The highly compact structures of lasso peptides confer a great resistance to chemical and proteolytic degradation as well as, in many cases, against thermally-induced unthreading [6-9]. The extraordinary mechanically interlocked topology of lasso peptides encompasses a large panel of functions, such as enzyme inhibitory, receptor antagonistic, antimicrobial or antiviral properties [1,10]. A limitation of the biological activity of lasso peptides is the unthreading of the C-terminal tail, a trend reported for several lasso peptides, yielding their corresponding branched-cyclic topoisomers [7-9,11].

BI-32169 is a class III lasso peptide produced by *Streptomyces* sp. that exerts a potent inhibitory activity against the human glucagon receptor [4,12]. To date, BI-32169 remains the only member of class III. BI-32169 features a nine residue macrolactam ring, generated by an isopeptide bond between the α-amino group of Gly1 and the side chain carboxyl group of Asp9 (highlighted in green in Figure 1), a loop of five residues (highlighted in blue) located above the ring, and a C-terminal tail of five residues (highlighted in orange) located below the ring. Its C-terminal part is sterically entrapped in the macrolactam ring by the Trp13 and Trp17 residues located on each side of the ring (highlighted in red in Figure 1). Additionally, the C-terminal Cys19 residue forms a disulfide bond with Cys6, which is located within the macrolactam ring, resulting in a

bicyclic primary structure (Figure 1). Nuclear magnetic resonance (NMR) was employed to unambiguously characterize the threading of the C-terminal tail through the macrolactam ring [4]. It has been proposed that the Pro12 and Pro16 residues of BI-32169 introduce two kinks resulting in a twisted S-like structure, in which the first kink, involving the Ile10-Trp13 residues, can be characterized as a type I β-turn. This sets the two cysteine residues in close proximity allowing the formation of the disulfide bond. However, NMR approaches require relatively large amounts of samples and the analysis of mixtures with the branched-cyclic topoisomer are not straightforward. MS-based approaches have been also applied as a tentative to elucidate lasso structures in the gas-phase. Cleavage within the C-terminal region of BI-32169 upon collision-induced dissociation (CID) [4,13] showed associated b_i and y_j product ions where a part of the C-terminal tail remains covalently linked to the macrolactam ring by the disulfide bond. However, these crosslinked product ions do not clearly constitute a signature of the lasso topology, as this type of fragment could also arise from its branched-cyclic topoisomer. Electron capture/transfer dissociation (EC/TD) [13,14] and ion mobility spectrometry – mass spectrometry (IMS-MS) [15,16] serve as an efficient alternative strategy for the identification of the lasso and branched-cyclic topologies.

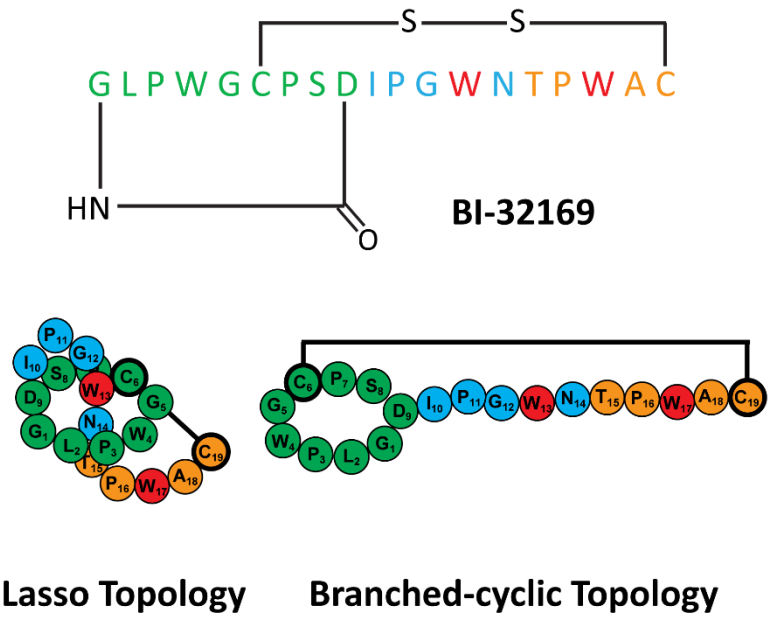

Figure 1. Sequences and schematics of the BI-32169 and its branched-cyclic analog. The macrolactam rings are colored in green, the loop residues in blue, the plugs in red and the C-terminal tail in orange. The disulfide bonds are shown by black lines.

In the present work, BI-32169 and its branched-cyclic topoisomer (Figure 1) were investigated using tandem mass spectrometry (CID and ECD) and trapped ion mobility spectrometry – mass spectrometry (TIMS-MS). The CID and ECD patterns as well as the TIMS-MS profiles of the two topologies of BI-32169 were compared for the first time to evidence specific structural signatures for lasso peptides containing disulfide bonds. In addition, the disulfide bond of BI-32169 was reduced/alkylated in order to derive information on the conformational changes in the absence of the disulfide bond and the lasso peptide was exposed to different temperatures in order to determine if the lasso structure is maintained in absence of the disulfide bond.

2. EXPERIMENTAL SECTION

2.1. Peptides and Sample Preparation. Details on BI-32169 production have been reported previously [4,12]. Briefly, *Streptomyces* sp. cells were grown in GYM medium at 28 °C for 5 days. BI-32169 was purified from the mycelium by extraction using methanol. The resulting extracts were directly subjected to reversed-phase high performance liquid chromatography (RP-HPLC) for purification. The branched-cyclic peptide of BI-32169 was obtained by solid-phase synthesis from Genepep (St Jean de Védas, France). The reduction of the disulfide bond of both peptides was carried out with 1 mM of tris(2-carboxyethyl)phosphine (TCEP) at 50 °C for 15 min. The alkylation was performed using 10 mM of N-ethylmaleimide (NEM) at room temperature for 15 min. Solutions were prepared at a final concentration of 5 µM in 10 mM ammonium acetate (NH_4Ac). To investigate the thermal stability of the BI-32169 and reduced/alkylated BI-32169, a solution of 10 µM of lasso peptide was incubated at 25 °C, 50 °C, 75 °C and 95 °C for 3 h. The same procedure was applied to the branched-cyclic analog of BI-32169 and the corresponding reduced/alkylated peptide as a control. Samples were subsequently analyzed via TIMS-MS. Low-concentration Tuning Mix calibration standard (TuneMix, G24221A) was purchased from Agilent Technologies (Santa Clara, CA). Details of the Tuning Mix structures is described elsewhere [17].

2.2. ECD Experiments. ECD experiments were carried out on a Solarix 7 T FT-ICR mass spectrometer (Bruker, Billerica, MA) equipped with a nanoESI source operating in the positive ion mode. Sample aliquots (10 µL) were loaded in a pulled-tip capillary to

the MS inlet. The ESI high voltage, capillary exit, and skimmers I and II were set to 1500 V, 200 V, 5 V and 16 V, respectively. ECD experiments were performed with a heated hollow cathode operating at a current of 1.6 A. Electrons emitted during 0.2 s were injected into the ICR cell with a 1.5 V bias and 16 V ECD lens.

2.3. Native TIMS-MS and CID Experiments. Details regarding the TIMS operation can be found elsewhere [18,19]. Briefly, Ion mobility experiments were performed on a custom built nanoESI-TIMS coupled to an Impact Q-TOF mass spectrometer (Bruker, Billerica, MA, Figure S2) [18]. The TIMS unit is controlled using a custom software in LabView (National Instruments) synchronized with the MS platform controls [19]. Sample aliquots (10 µL) were loaded in a pulled-tip capillary biased at 700-1500 V relative to the MS inlet. TIMS separation is based on holding the ions stationary using an electric field (E) against a moving buffer gas (Figure S2) [20]. In TIMS operation, multiple isomers/conformers are trapped simultaneously at different E values resulting from a voltage gradient applied across the IMS tunnel region (Figure S2). Mobility selected ions are then eluted from the TIMS analyzer region by decreasing the electric field (Figure S2). TIMS separation was carried out using nitrogen (N_2) as buffer gas at room temperature (T). The v_g is set by the pressure difference between the funnel entrance ($P1$ = 2.6 mbar) and exit ($P2$ = 1.1 mbar, Figure S2). An rf voltage of 250 V_{pp} at 880 kHz was applied to all electrodes. Separations were performed using with a voltage ramp (V_{ramp}) of -250 to -100 V, deflector voltage (V_{def}) of 60 V and base voltage (V_{out}) of 60 V. TIMS separation depends on the gas flow velocity (v_g), elution voltage ($V_{elution}$), ramp time (t_{ramp}) and base voltage (V_{out}) [18,20]. The reduced mobility, K_o, is defined by:

$$K_0 = \frac{v_g}{E} \cong \frac{A}{(V_{elution} - V_{out})} \quad (1)$$

The constant A was determined using known reduced mobilities of calibration standards (Tuning Mix) [17]. The elution voltage was determined experimentally by varying the ramp time for a constant ramp voltage as describe elsewhere [17]. The measured mobilities were converted into collision cross sections (CCS, Å^2) using the Mason-Schamp equation:

$$\Omega = \frac{(18\pi)^{1/2}}{16} \frac{q}{(k_B T)^{1/2}} \left(\frac{1}{m} + \frac{1}{M}\right)^{1/2} \frac{1}{N} \times \frac{1}{K} \quad (3)$$

where q is the ion charge, k_B is the Boltzmann constant, N is the gas number density, m is the ion mass, and M is the gas molecule mass [20].

Collision induced dissociation (CID) experiments were performed in the collision cell located after the TIMS analyzer (Figure S2). The mass-selected $[M+2H]^{2+}$ ions were fragmented using nitrogen as collision gas at a collision energy of 26 V. The mobility resolving power (R) and the resolution (r) are defined as $R = \Omega/w$ and $r = 1.18*(\Omega_2-\Omega_1)/(w_1+w_2)$, where w is the full peak width at half maximum (FWHM).

3. RESULTS AND DISCUSSION

3.1. CID Fragmentation Pattern of BI-32169. The CID spectra of the doubly protonated species of the class III lasso peptide BI-32169 (m/z 1018.9) and its branched-cyclic topoisomer are illustrated in Figure 2a and 2b, respectively. The CID spectrum of BI-32169 displayed a complicated fragmentation pattern due to the presence of the disulfide bond (Figure 2a). The disulfide bond linking the C-terminus to the macrolactam ring prevents the formation of classic b_i/y_j series. However, cross-linked product ions from b_i and y_j ions, denoted as $[(b_i)^-(y_j)]$, were observed. These fragments result from two bond cleavages in the C-terminal part, where a part of the C-terminal tail remains covalently linked to the macrolactam ring by the disulfide bond as illustrated in Figure 2a. Such cross-linked species were also previously observed for the class I lasso peptides sviceucin and siamycin I which contain two disulfide bonds [13]. The present cross-linked product ions are different from the mechanically interlocked fragments, denoted as $[(b_i)^*(y_j)]$, previously observed for class II lasso peptides, where b_i and y_j ions remain associated through steric interactions imparted by bulky residues, which entrap the C-terminal tail inside the macrolactam ring [13]. The main cross-linked product ions observed for BI-32169 were $[(b_9)^-(y_9)]^{2+}$, $[(b_{10})^-(y_2)]$, $[(b_{10})^-(y_4)]$ and $[(b_{10})^-(y_5)]$, associated with their complementary internal fragment ions $(b_{10}y_{10})_1$, $(b_{17}y_9)_7$, $(b_{15}y_9)_5$ and $(b_{14}y_9)_4$, respectively. The presence of a disulfide bond in the lasso structure could also explain the formation of many internal product ions (Figure 2a).

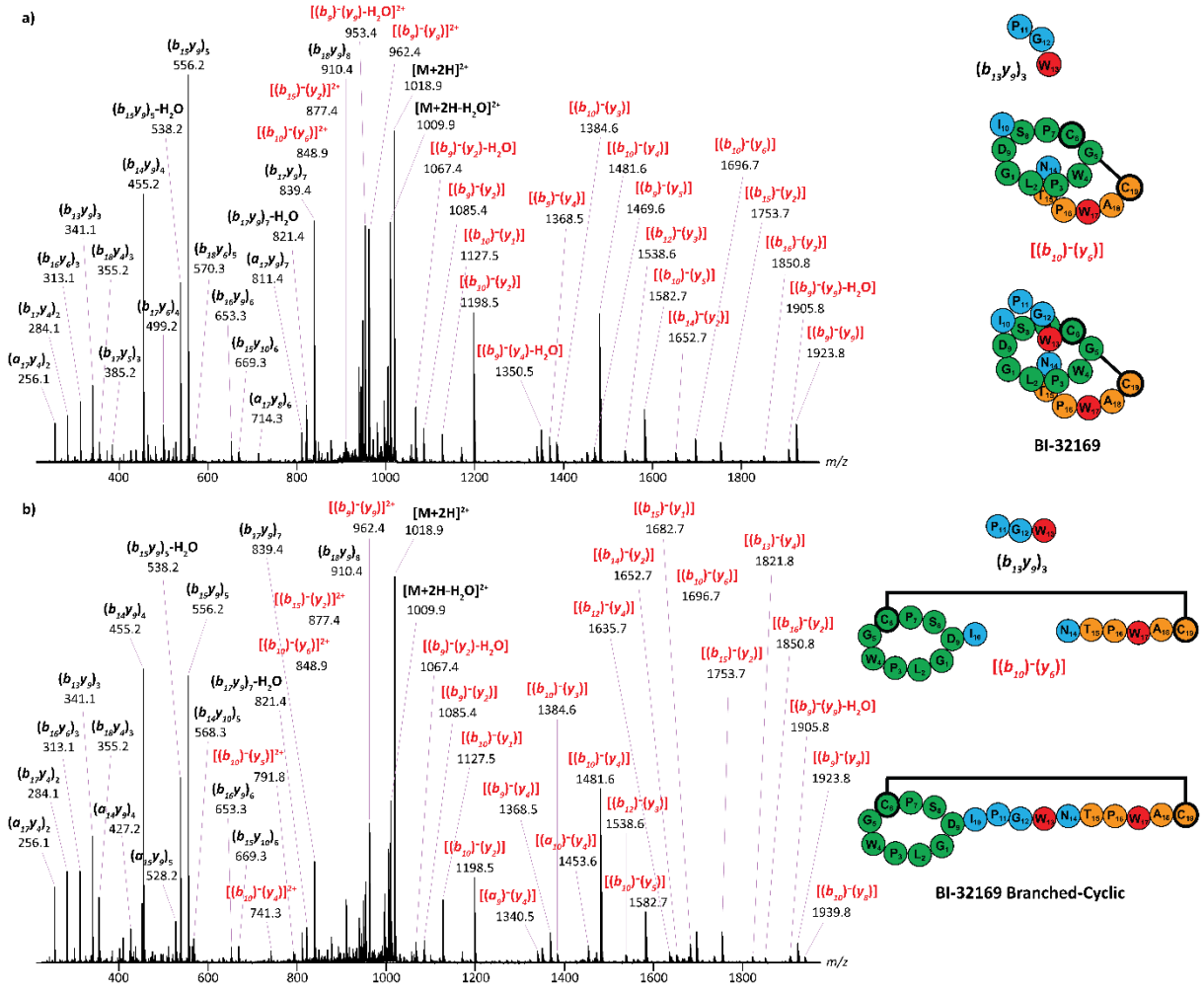

Figure 2. CID spectra of the doubly protonated species of (a) BI-32169 and (b) its branched-cyclic topoisomer (*m/z* 1018.9). Typical cross-linked product ions are highlighted in red and labeled on the peptide cartoons (right of each panel). The macrolactam rings, the loop residues, the plugs, the C-terminal tails and the disulfide bonds are highlighted in green, blue, red, orange and black, respectively.

The CID spectrum of the doubly protonated species of the branched-cyclic analog of BI-32169 exhibited a similar fragmentation pattern as compared to the lasso structure (Figure 2b). The same cross-linked product ions and internal fragments were observed for the two topologies. Contrary to class II lasso peptides, for which lasso-specific mechanically interlocked fragments are observed, the CID experiment of BI-32169 is less informative as the cross-linked products occur for the branched-cyclic analog of BI-32169 as well (Figure 2). Thus, CID experiments are not suitable to determine structural signatures for the lasso topology of class I and III lasso peptides containing disulfide bonds.

3.2. ECD Fragmentation Pattern of BI-32169. We previously demonstrated the utility of ETD for identifying class II lasso peptide topologies as an alternative fragmentation approach to overcome the limited structural information provided by CID experiments [13]. The class III lasso peptide BI-32169 and its branched-cyclic analog displayed very close fragmentation patterns in ECD for the doubly protonated species (Figure 3). Both topologies presented the charge-reduced $[M+2H]^{\bullet+}$ ions (m/z 2037.9) as the most abundant species. ECD has been showed to be very powerful for biomolecules containing disulfide bonds as the capture of a single electron can induce a dissociation of both backbone and disulfide bonds [21,22]. In fact, $c'_i/z_j^{\bullet}$ series were observed, consisting of c'_{12} to c'_{18} (except c'_{15}) together with their complementary $z_7^{\bullet}$ to $z_1^{\bullet}$ (except $z_4^{\bullet}$), that involve the cleavage of the disulfide bond between Cys6 and Cys19 concomitant with backbone cleavages within the C-terminal part of both topologies (Figure 3). As previously mentioned for class II lasso peptides [13,14], significantly different relative abundance was observed for the fragments only comprising the macrolactam ring. Indeed, the branched-cyclic analog of BI-32169 exhibited abundant c'_9 and $z_{10}^{\bullet}$ fragments (Figure 3b) while $z_{10}^{\bullet}$ and c'_9 were much smaller and absent, respectively, for the lasso structure (Figure 3a). This difference probably means that the two complementary c'_9 and $z_{10}^{\bullet}$ fragments remained sterically interlocked in the lasso topology.

As with class II lasso peptides [13,14], ECD spectra of BI-32169 displayed an increase of hydrogen migration events near the loop region (Ile10-Asn14) when compared to the branched-cyclic topoisomer, as illustrated in Figure 3c. In fact, BI-32169 showed fragment ions involving extensive hydrogen migration within $c_{12}^{\bullet}$ to $c_{14}^{\bullet}$ and their complementary z'_7 to z'_5 product ions (highlighted in red in Figure 3) while these fragments were lower in relative intensity for the branched-cyclic topology, indicating that the hydrogen migration events in the Ile10-Asn14 region occur less frequently in the absence of a lasso structure (Figure 3c). Contrary to CID, where BI-32169 and the branched-cyclic topoisomer present similar fragmentation patterns, ECD enables specific structural signatures for the class III lasso peptide BI-32169 through the presence of extensive hydrogen migrations. As a consequence, the combination of the present results with a previous study [13] enables us to firmly propose that ECD can be used to characterize lasso topologies regardless of the lasso peptide class and the size of the loop,

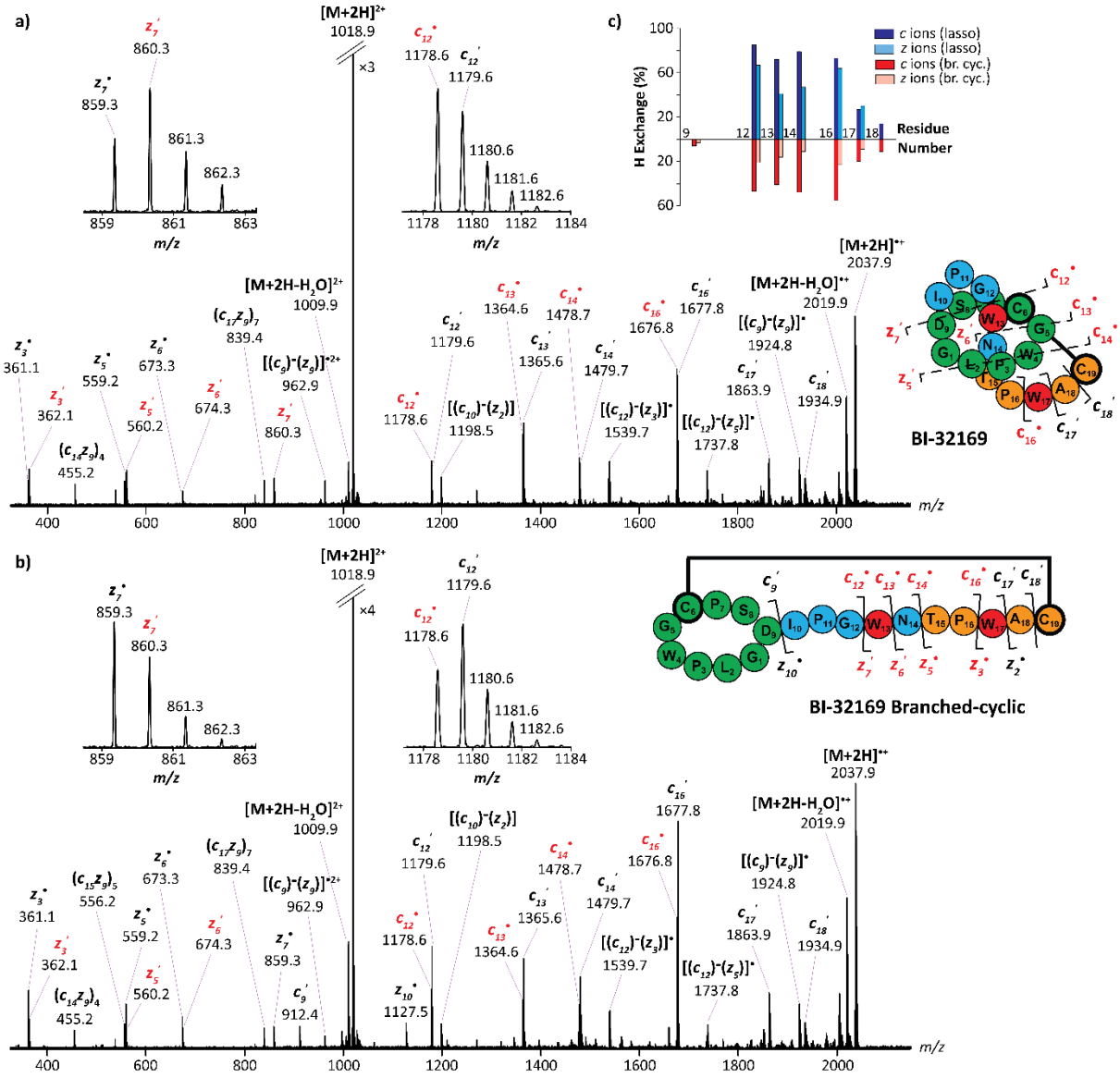

Figure 3. ECD spectra of the doubly protonated species of (a) BI-32169 and (b) the branched-cyclic topoisomer (*m/z* 1018.9). Typical hydrogen migration events are highlighted in red and labeled on the peptide cartoons (right of each panel). (c) Bar plot showing the hydrogen migration events of BI-32169 (blue bars) and the branched-cyclic topoisomer (red bars) obtained by comparison between the experimental and theoretical isotope patterns. The macrolactam rings, the loop residues, the plugs, the C-terminal tails and the disulfide bonds are highlighted in green, blue, red, orange and black, respectively.

and in differentiating lasso peptides from their unthreaded branched-cyclic topoisomers. However, the differences in the hydrogen migration events were less pronounced as previously observed for class II lasso peptides [13]. This could be explained by the presence of the disulfide bond that links the macrolactam ring to the

C-terminus, which imposes additional constraints for the branched-cyclic topoisomer of BI-32169 by fixing the C-terminal part in closer proximity to the macrolactam ring. This feature facilitates hydrogen migration events more strongly than the completely unstructured C-terminal part in the branched-cyclic analogs of class II lasso peptides.

3.3. Native nESI-TIMS-MS Analysis of BI-32169. We demonstrated the utility of the ECD approach to evidence specific structural signatures for lasso peptides containing disulfide bonds. However, the less pronounced differences in the hydrogen migration events combined with the limited application for the case of mixtures caused us to consider TIMS-MS as a complementary strategy. TIMS-MS proved very effective for the characterization of class II lasso peptides and in differentiating them from their unthreaded branched-cyclic topoisomers [15,16]. Native TIMS spectra corresponding to the doubly protonated species of BI-32169 and its branched-cyclic topoisomer are presented in Figure 4a. The collision cross sections (CCS) and resolving power (R) metrics are listed in Table S1. Previous traveling wave IMS (TWIMS) experiments showed a single broad arrival time distribution ($R \sim 15$) for the doubly protonated species of BI-32169 (Figure S3) [23]. By contrast, the high mobility resolving power ($R \sim$ 70–200) achieved by using TIMS at fast scan rates (Sr = 0.3 V/ms) resulted in the identification of multiple IMS bands for the two topoisomers, providing additional information on the conformational spaces adopted during native conditions, as previously shown for the lasso topology of BI-32169 [15] (Figure 4a). In addition, the multiple IMS bands of BI-32169 cover a relatively large CCS region as compared to the class II lasso peptides [15], suggesting that the disulfide bond prevents the peptide from collapsing to more compact structures. We previously demonstrated that the branched-cyclic topologies adopt significantly more extended structures than the class II lasso peptides, permitting a clear separation of the two topoisomers in native TIMS-MS using fast scan rates (Sr = 0.3-0.56 V/ms) [15]. In the case of the branched-cyclic analog of BI-32169, the multiple conformations were just slightly more extended than the lasso topology, suggesting that the disulfide bond prevents the peptide from

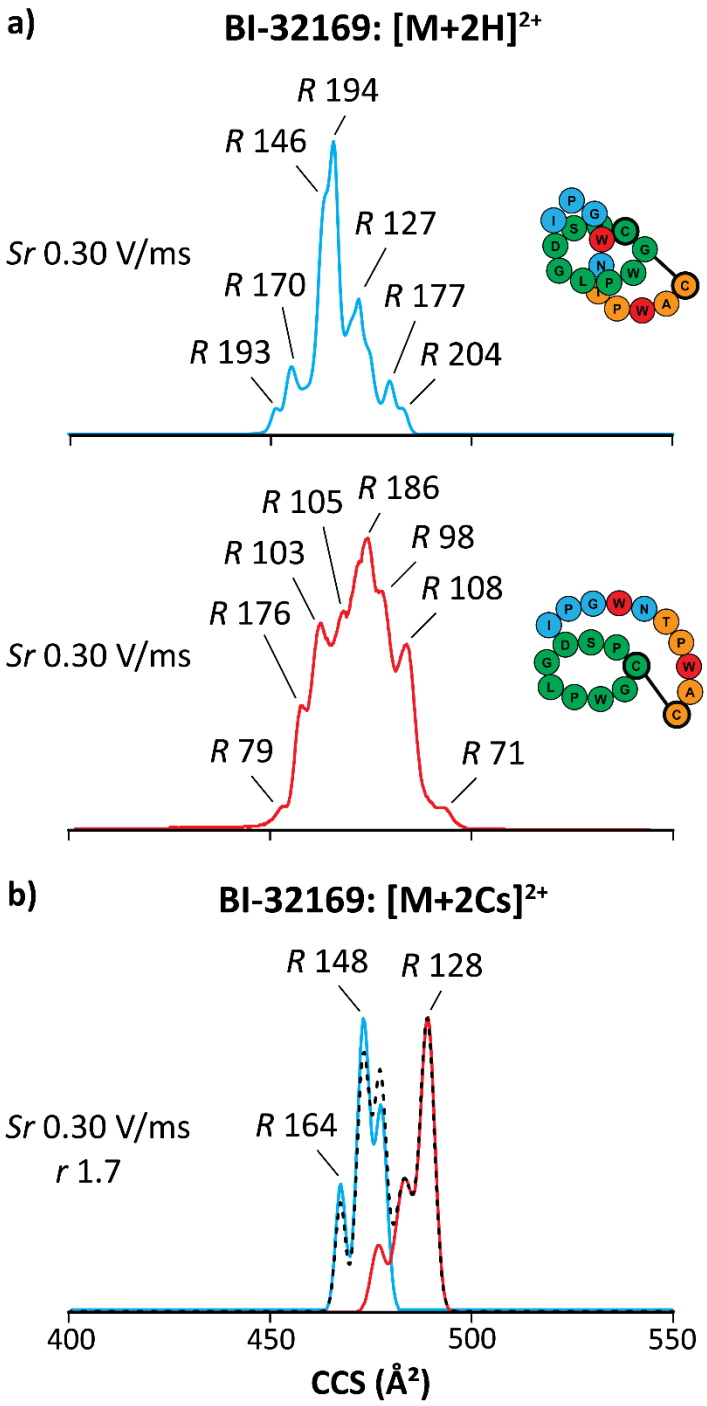

Figure 4. TIMS spectra of (a) the doubly protonated species and (b) the doubly cesiated species of BI-32169 (blue traces) and its branched-cyclic topoisomer (red traces). The dashed line represents the TIMS profile of both topoisomers in mixture. Schemes highlight the macrolactam rings in green, the loop residues in blue, the plugs in red and the C-terminal tail in orange. The disulfide bonds are represented by black lines. The *R*, *r*, and *Sr* values are given.

extending of the unthreaded C-terminal part (Figure 4a). As a consequence, the lasso and branched-cyclic topoisomers of BI-32169 were not clearly separated for the doubly protonated species.

The use of metalation, especially the doubly cesiated species, has been shown to be very powerful in reducing the conformational space (i.e., number of IMS bands) via intramolecular complexation as well as to separate lasso and branched-cyclic topologies (see examples in a previous report of metalation of class II lasso peptides [15,24]). The effect of the doubly cesiated species on the TIMS separation of BI-32169 and its branched-cyclic topoisomer is illustrated in Figure 4b and the measured collision cross sections (CCS) and resolving power (R) metrics are listed in Table S1. Inspection of Figure 4b shows that the doubly cesiated species resulted in better mobility separation ($r \sim 1.7$) at fast scan rates between BI-32169 and its branched-cyclic topoisomer. In addition, the use of cesium metal ions permitted to considerably reduce the number of conformations for both topoisomers (Figure 4b). Contrary to the class II lasso peptides, the doubly cesiated species of BI-32169 displayed three distinct IMS bands at similar CCS, suggesting that the disulfide bond imposes strong constraints to the structure making the lasso topology of BI-32169 very rigid; even the introduction of a metal ion with a large ionic radius barely extended the lasso structure. In the case of the doubly cesiated species of the branched-cyclic analog of BI-32169, three distinct IMS bands, including two compact minor conformations, were observed indicating that the disulfide bond prevents the peptide from completely extending the unthreaded C-terminal part, even when introducing a metal ion with a large ionic radius.

The disulfide bonds of the two BI-32169 topoisomers were reduced and alkylated in order to assess the conformational changes of the loss of the disulfide bond on the lasso and branched-cyclic structures. The effect of the reduction and alkylation of the disulfide bonds of BI-32169 and its branched-cyclic topoisomer is presented in Figure 5a and the measured collision cross sections (CCS) and resolving power (R) metrics are listed in Table S1. The reduced/alkylated BI-32169 and the branched-cyclic analog exhibited different mobility profiles, indicating that the lasso structure is preserved even when losing the disulfide bond. The high mobility resolving power ($R \sim 75–235$) also resulted in the identification of multiple conformations for the two reduced and alkylated

topoisomers. However, the major IMS band of the reduced/alkylated BI-32169 was observed at significantly higher CCS (~ +30 Å²) as compared to the major IMS band of the doubly protonated species of BI-32169 (Figures 4a and 5a). In fact, a low CCS difference (~ +8 Å²) was obtained by comparing the major IMS band of the doubly protonated and cesiated species of BI-32169. This means that the loss of the disulfide

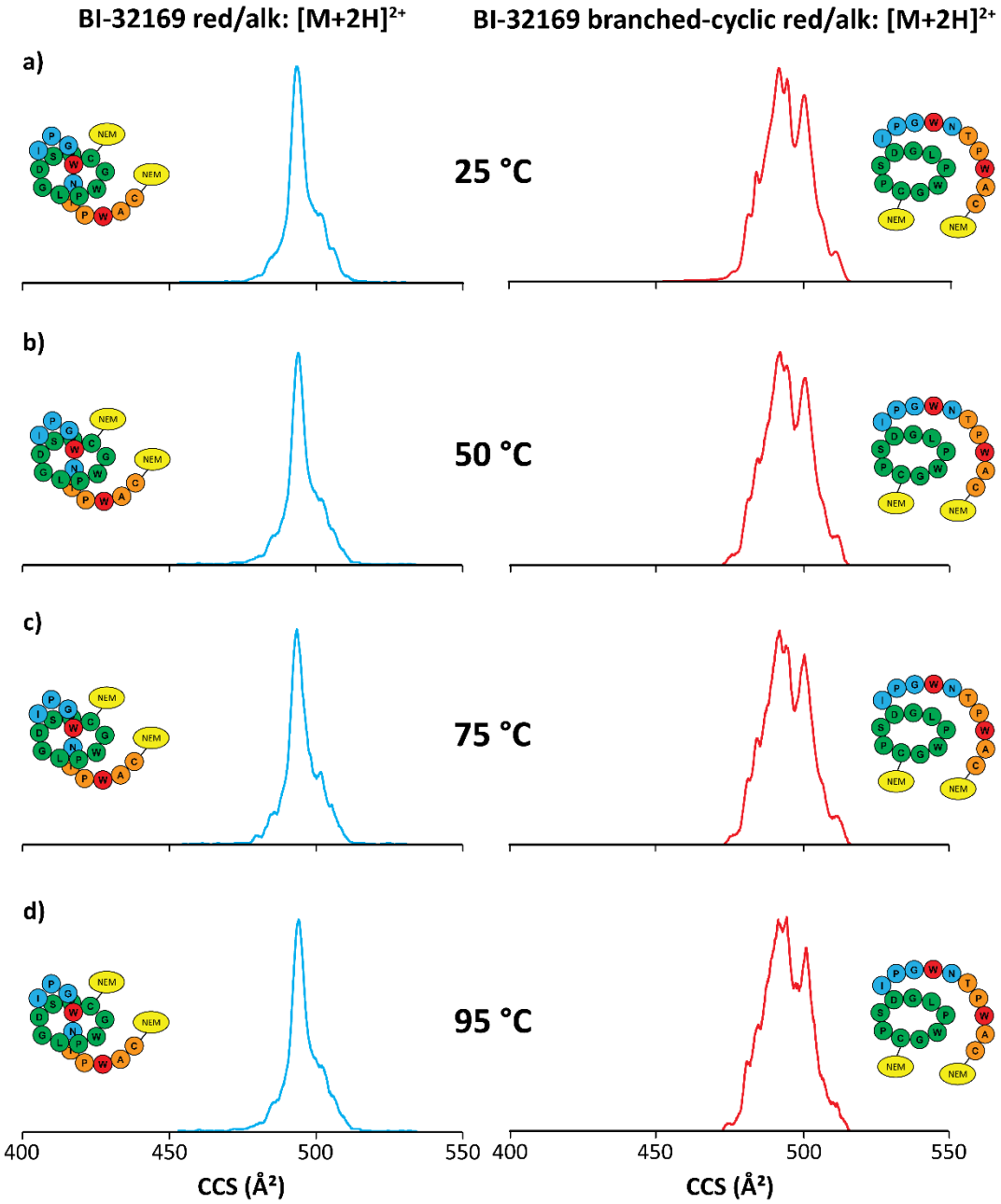

Figure 5. TIMS spectra (*Sr* = 0.3 V/ms) of the doubly protonated species of the reduced/alkylated BI-32169 (blue traces) and the corresponding branched-cyclic peptide (red traces) at (a) 25 °C, (b) 50 °C, (c) 75 °C and (d) 95 °C. Schemes highlight the

macrolactam rings in green, the loop in blue, the plugs in red and the C-terminal tail in orange. The alkylating reagents (NEM) are represented in yellow.

bond makes the C-terminal tail of the reduced/alkylated BI-32169 more flexible and induces an expansion of the lasso structure. The corresponding branched-cyclic peptide exhibited two major conformations, for which more extended structures were observed as compared to the main conformations of the branched-cyclic analog of BI-32169 (Figures 4a and 5a). This indicates an unfolding of the free C-terminal tail due to the absence of the disulfide bond. Nevertheless, this trend was less pronounced for the main compact structures when compared to the lasso structure, as reflected by the smaller CCS difference (~ +15 $Å^2$) between the branched-cyclic analog of BI-32169 and its reduced/alkylated form, even adopting an overall topology close to the reduced/alkylated BI-32169. This suggests that the free C-terminal tail of the reduced/alkylated branched-cyclic analog of BI-32169 can also be folded probably by making intramolecular interactions between the flexible C-terminal tail and the macrolactam ring.

3.4. Thermal Stability of BI-32169. As a consequence of their compact and interlocked structures, many lasso peptides exhibit an outstanding stability toward thermal unthreading [7,11,25-27]. However, several lasso peptides have been reported to unfold at high temperature into their branched-cyclic topoisomers [7,8,26,28]. These findings encouraged us to study the thermostability of BI-32169 and the reduced/alkylated form of BI-32169. The effect of the temperature on the conformational space of BI-32169 and BI-32169 reduced/alkylated together with their respective branched-cyclic topoisomers are illustrated in Figures S4 and 5, respectively. The TIMS experiments carried out on the branched-cyclic peptides served as a control of the unfolding of the lasso topologies. Similar TIMS profiles were observed when BI-32169 was subjected to solution temperatures of 25 °C, 50 °C, 75 °C and 95 °C for 3 h (Figure S4). This suggests that BI-32169 can withstand prolonged exposure to high temperature. Because of the strong heat stability of BI-32169, the reduced/alkylated form of BI-32169, which has been demonstrated to be less rigid, was also subjected to the same treatment (solution temperatures of 25 °C, 50 °C, 75 °C and 95 °C for 3 h, Figure 5). As for BI-32169, the reduced/alkylated form displayed similar TIMS profiles under these conditions, indicating that the lasso structure is preserved and therefore heat stable. This suggests

that the two bulky residues Trp13 and Trp17, which are located above and below the ring respectively, are sufficient to maintain the lasso topology even at highly elevated temperatures.

4. CONCLUSION

Herein, mass spectrometry experiments were performed for the first time on a lasso peptide containing a disulfide bond together with the corresponding branched-cyclic topoisomer to find specific structural signatures of the two topologies. The CID experiments showed similar fragmentation pattern for the two topologies, where a part of the C-terminal tail remains covalently linked to the macrolactam ring by the disulfide bond. As these cross-linked product ions also occurred for the branched-cyclic topology, CID did not revealed specific signatures of the lasso topology of BI-32169. That is, CID experiments are only effective for class II lasso peptides in which the loop region is five residues or longer.

ECD experiments with BI-32169 showed a larger extent of hydrogen migration near the loop region, when compared to the branched-cyclic topoisomer, providing evidence of specific structural signatures for the lasso topology. Note that the differences in the hydrogen migration events of BI-32169 and the branched-cyclic topoisomer are less pronounced, when compared to the class II lasso peptides, due to the presence of the disulfide bond which imposes additional constraints to the two topologies. These results suggest that ECD can be efficient to characterize lasso peptides regardless of the class and loop region size, and to differentiate the lasso topologies from their unthreaded branched-cyclic topoisomers.

The potential of native nESI-TIMS-MS for identifying the class III lasso peptide BI-32169 from the branched-cyclic topoisomers is illustrated for the doubly protonated species. The lasso and branched-cyclic topologies of BI-32169 are clearly separated when complexed with cesium metal ions due to the reduction on the conformational space, and not when in complex with sodium and potasium. The present TIMS-MS data on lasso peptide containing disulfide bond combined with a previous work on class II lasso peptides (without disulfide bond) [24], allow to strongly propose that the metal cesium ions can be used to clearly separate any lasso peptide from its branched-cyclic

topoisomers regardless the class and loop size. We also showed the thermally stable behavior of BI-32169 and evidenced conformational changes by reducing and alkylating the disulfide bond of BI-32169. This provides new insights about the presence of the disulfide bond in the lasso structure which probably has a crucial role in the inhibitory activity against the human glucagon receptor.

ACKNOWLEDGMENTS

The authors acknowledge the financial support from the National Science Foundation Division of Chemistry, under CAREER award CHE-1654274, with co-funding from the Division of Molecular and Cellular Biosciences to FFL. J. D. H. thanks the Deutsche Forschungsgemeinschaft for financial support (DFG Research Fellowship 309199717).

AUTHOR CONTRIBUTIONS

The manuscript was written through contributions of all authors. All authors have given approval to the final version of the manuscript.

Competing Interests

The authors declare no competing interests.

REFERENCES

1. Hegemann JD, Zimmermann M, Xie X, Marahiel MA (2015) Lasso peptides: an intriguing class of bacterial natural products. Acc Chem Res 48 (7):1909-1919. doi:10.1021/acs.accounts.5b00156

2. Rosengren KJ, Clark RJ, Daly NL, Goeransson U, Jones A, Craik DJ (2003) Microcin J25 Has a Threaded Sidechain-to-Backbone Ring Structure and Not a Head-to-Tail Cyclized Backbone. J Am Chem Soc 125:12464-12474. doi:10.1021/ja0367703

3. Li Y, Ducasse R, Zirah S, Blond A, Goulard C, Lescop E, Giraud C, Hartke A, Guittet E, Pernodet JL, Rebuffat S (2015) Characterization of Sviceucin from Streptomyces Provides Insight into Enzyme Exchangeability and Disulfide Bond Formation in Lasso Peptides. ACS Chem Biol 10 (11):2641-2649. doi:10.1021/acschembio.5b00584

4. Knappe TA, Linne U, Xie X, Marahiel MA (2010) The glucagon receptor antagonist BI-32169 constitutes a new class of lasso peptides. FEBS Lett 584 (4):785-789. doi:10.1016/j.febslet.2009.12.046

5. Tietz JI, Schwalen CJ, Patel PS, Maxson T, Blair PM, Tai HC, Zakai UI, Mitchell DA (2017) A new genome-mining tool redefines the lasso peptide biosynthetic landscape. Nat Chem Biol 13 (5):470-478. doi:10.1038/nchembio.2319
6. Ducasse R, Yan KP, Goulard C, Blond A, Li Y, Lescop E, Guittet E, Rebuffat S, Zirah S (2012) Sequence determinants governing the topology and biological activity of a lasso peptide, microcin J25. ChemBioChem 13 (3):371-380. doi:10.1002/cbic.201100702
7. Hegemann JD, Zimmermann M, Zhu S, Klug D, Marahiel MA (2013) Lasso peptides from proteobacteria: Genome mining employing heterologous expression and mass spectrometry. Biopolymers 100 (5):527-542. doi:10.1002/bip.22326
8. Zimmermann M, Hegemann JD, Xie X, Marahiel MA (2013) The astexin-1 lasso peptides: biosynthesis, stability, and structural studies. Chem Biol 20 (4):558-569. doi:10.1016/j.chembiol.2013.03.013
9. Hegemann JD, Fage CD, Zhu S, Harms K, Di Leva FS, Novellino E, Marinelli L, Marahiel MA (2016) The ring residue proline 8 is crucial for the thermal stability of the lasso peptide caulosegnin II. Mol Biosyst 12 (4):1106-1109. doi:10.1039/c6mb00081a
10. Maksimov MO, Pan SJ, James Link A (2012) Lasso peptides: structure, function, biosynthesis, and engineering. Nat Prod Rep 29 (9):996-1006. doi:10.1039/c2np20070h
11. Knappe TA, Linne U, Robbel L, Marahiel MA (2009) Insights into the biosynthesis and stability of the lasso peptide capistruin. Chem Biol 16 (12):1290-1298. doi:10.1016/j.chembiol.2009.11.009
12. Potterat O, Wagner K, Gemmecker G, Mack J, Puder C, Vettermann R, Streicher R (2004) BI-32169, a bicyclic 19-peptide with strong glucagon receptor antagonist activity from Streptomyces sp. J Nat Prod 67 (9):1528-1531. doi:10.1021/np0400930
13. Jeanne Dit Fouque K, Lavanant H, Zirah S, Hegemann JD, Fage CD, Marahiel MA, Rebuffat S, Afonso C (2018) General rules of fragmentation evidencing lasso structures in CID and ETD. Analyst 143 (5):1157-1170. doi:10.1039/c7an02052j
14. Perot-Taillandier M, Zirah S, Rebuffat S, Linne U, Marahiel MA, Cole RB, Tabet JC, Afonso C (2012) Determination of peptide topology through time-resolved double-resonance under electron capture dissociation conditions. Anal Chem 84 (11):4957-4964. doi:10.1021/ac300607y
15. Dit Fouque KJ, Moreno J, Hegemann JD, Zirah S, Rebuffat S, Fernandez-Lima F (2018) Identification of Lasso Peptide Topologies Using Native Nanoelectrospray Ionization-

Trapped Ion Mobility Spectrometry-Mass Spectrometry. Anal Chem 90 (8):5139-5146. doi:10.1021/acs.analchem.7b05230

16. Jeanne Dit Fouque K, Afonso C, Zirah S, Hegemann JD, Zimmermann M, Marahiel MA, Rebuffat S, Lavanant H (2015) Ion mobility-mass spectrometry of lasso peptides: signature of a rotaxane topology. Anal Chem 87 (2):1166-1172. doi:10.1021/ac503772n

17. Hernandez DR, Debord JD, Ridgeway ME, Kaplan DA, Park MA, Fernandez-Lima F (2014) Ion dynamics in a trapped ion mobility spectrometer. Analyst 139 (8):1913-1921. doi:10.1039/c3an02174b

18. Fernandez-Lima FA, Kaplan DA, Suetering J, Park MA (2011) Gas-phase separation using a Trapped Ion Mobility Spectrometer. Int J Ion Mobil Spectrom 14 (2-3):93-98

19. Fernandez-Lima FA, Kaplan DA, Park MA (2011) Note: Integration of trapped ion mobility spectrometry with mass spectrometry. Rev Sci Instrum 82 (12):126106. doi:10.1063/1.3665933

20. McDaniel EW, Mason EA (1973) Mobility and diffusion of ions in gases. Wiley Series in Plasma Physics. John Wiley and Sons, Inc., New York, New York

21. Zubarev RA, Kruger NA, Fridriksson EK, Lewis MA, Horn DM, Carpenter BK, McLafferty FW (1999) Electron Capture Dissociation of Gaseous Multiply-Charged Proteins Is Favored at Disulfide Bonds and Other Sites of High Hydrogen Atom Affinity. J Am Chem Soc 121 (12):2857-2862. doi:10.1021/ja981948k

22. Ganisl B, Breuker K (2012) Does Electron Capture Dissociation Cleave Protein Disulfide Bonds? ChemistryOpen 1 (6). doi:10.1002/open.201200038

23. Fouque KJ, Lavanant H, Zirah S, Hegemann JD, Zimmermann M, Marahiel MA, Rebuffat S, Afonso C (2017) Signatures of Mechanically Interlocked Topology of Lasso Peptides by Ion Mobility-Mass Spectrometry: Lessons from a Collection of Representatives. J Am Soc Mass Spectrom 28 (2):315-322. doi:10.1007/s13361-016-1524-8

24. Jeanne Dit Fouque K, Moreno J, Hegemann JD, Zirah S, Rebuffat S, Fernandez-Lima F (2018) Metal ions induced secondary structure rearrangements: mechanically interlocked lasso vs. unthreaded branched-cyclic topoisomers. Analyst 143 (10):2323-2333. doi:10.1039/c8an00138c

25. Salomon RA, Farias RN (1992) Microcin 25, a novel antimicrobial peptide produced by Escherichia coli. J Bacteriol 174 (22):7428-7435

26. Hegemann JD, Zimmermann M, Xie X, Marahiel MA (2013) Caulosegnins I-III: a highly diverse group of lasso peptides derived from a single biosynthetic gene cluster. J Am Chem Soc 135 (1):210-222. doi:10.1021/ja308173b

27. Hegemann JD, Zimmermann M, Zhu S, Steuber H, Harms K, Xie X, Marahiel MA (2014) Xanthomonins I-III: a new class of lasso peptides with a seven-residue macrolactam ring. Angew Chem Int Ed Engl 53 (8):2230-2234. doi:10.1002/anie.201309267

28. Allen CD, Chen MY, Trick AY, Le DT, Ferguson AL, Link AJ (2016) Thermal Unthreading of the Lasso Peptides Astexin-2 and Astexin-3. ACS Chem Biol 11 (11):3043-3051. doi:10.1021/acschembio.6b00588.

FIGURES

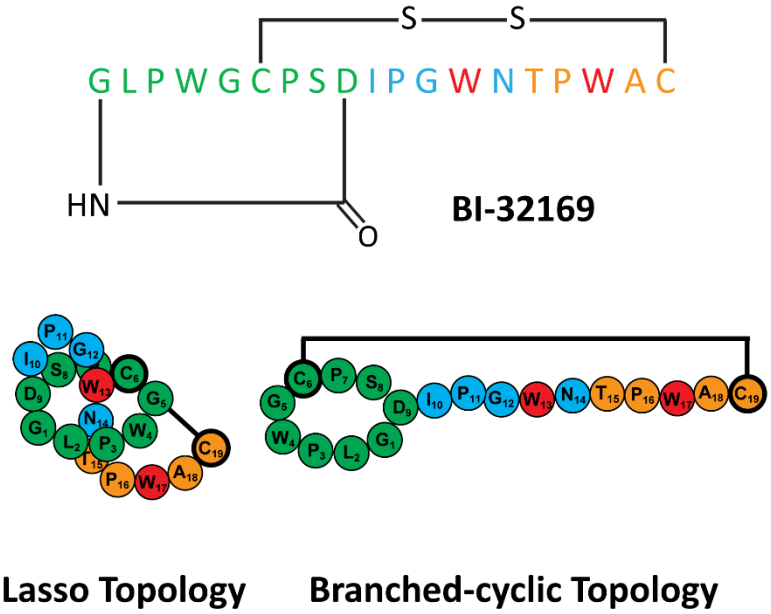

Figure 1. Sequences and schematics of the BI-32169 and its branched-cyclic analog. The macrolactam rings are colored in green, the loop residues in blue, the plugs in red and the C-terminal tail in orange. The disulfide bonds are shown by black lines.

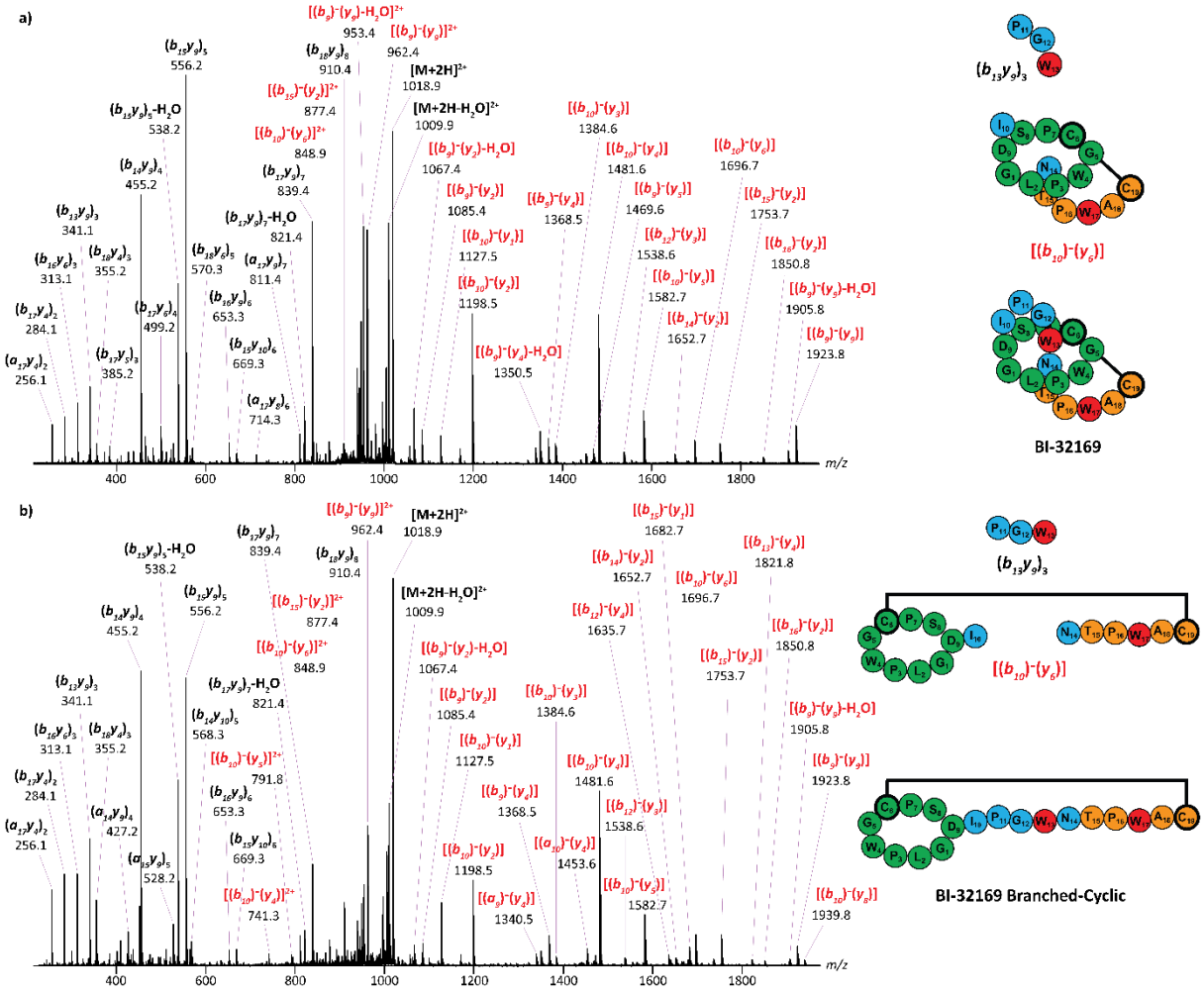

Figure 2. CID spectra of the doubly protonated species of (a) BI-32169 and (b) its branched-cyclic topoisomer (*m/z* 1018.9). Typical cross-linked product ions are highlighted in red and labeled on the peptide cartoons (right of each panel). The macrolactam rings, the loop residues, the plugs, the C-terminal tails and the disulfide bonds are highlighted in green, blue, red, orange and black, respectively.

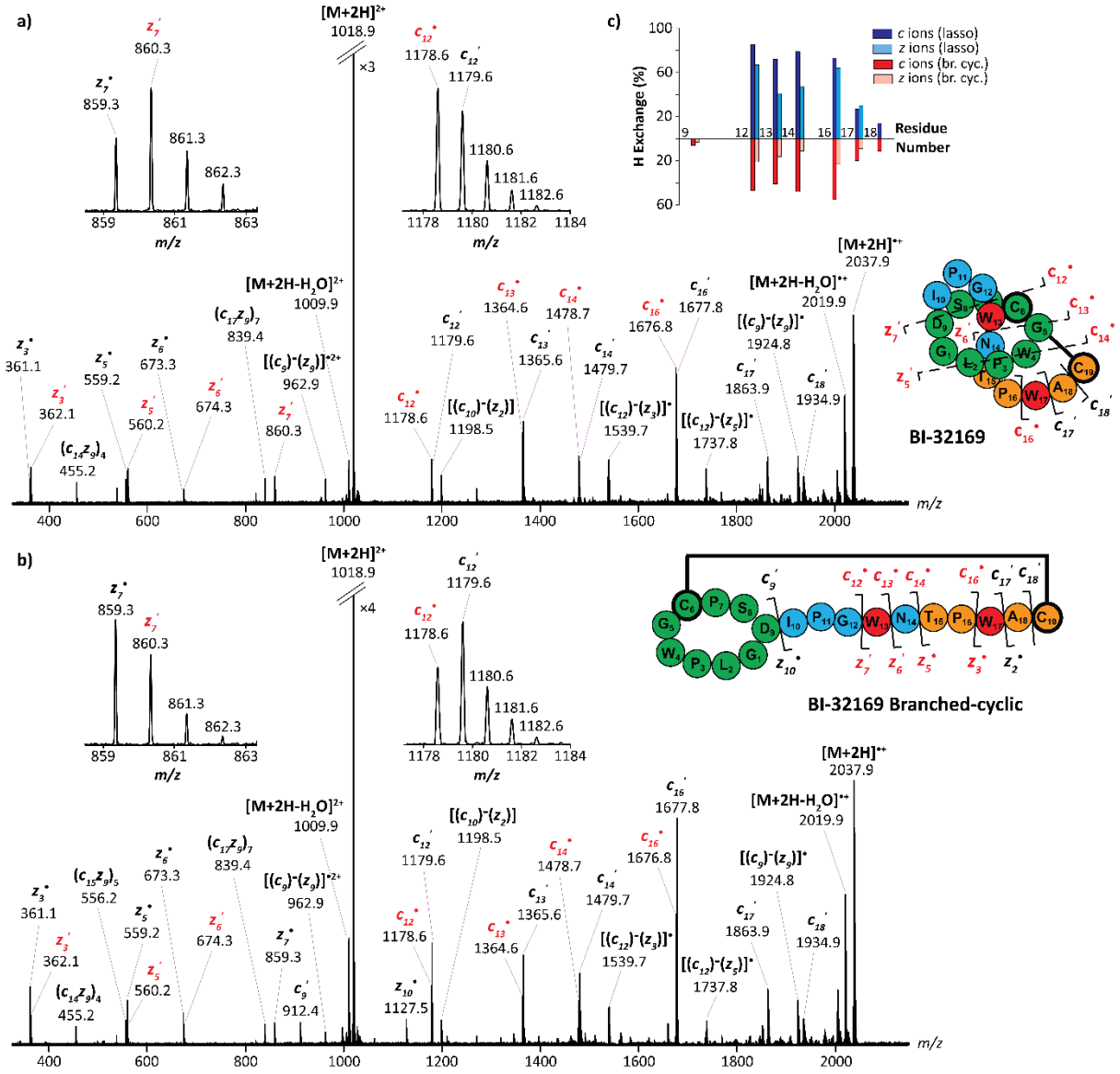

Figure 3. ECD spectra of the doubly protonated species of (a) BI-32169 and (b) the branched-cyclic topoisomer (*m/z* 1018.9). Typical hydrogen migration events are highlighted in red and labeled on the peptide cartoons (right of each panel). (c) Bar plot showing the hydrogen migration events of BI-32169 (blue bars) and the branched-cyclic topoisomer (red bars) obtained by comparison between the experimental and theoretical isotope patterns. The macrolactam rings, the loop residues, the plugs, the C-terminal tails and the disulfide bonds are highlighted in green, blue, red, orange and black, respectively.

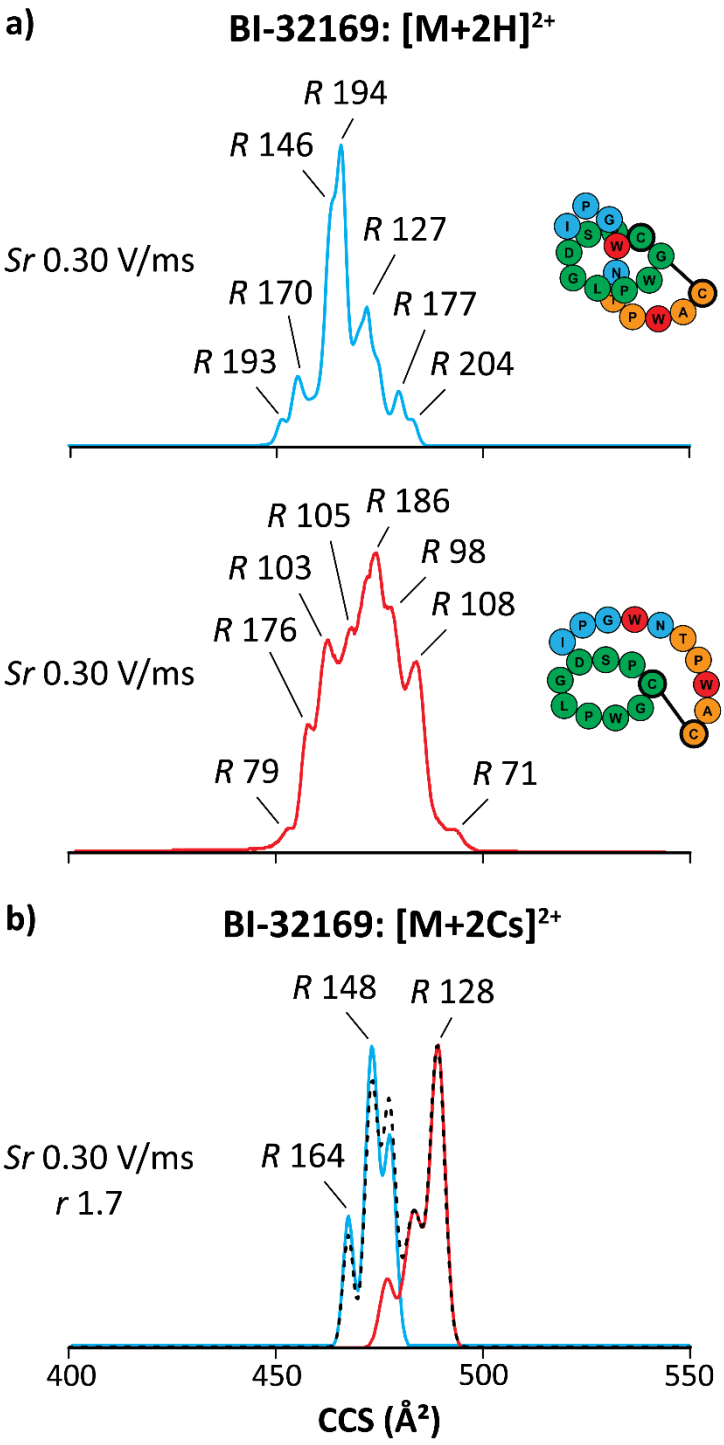

Figure 4. TIMS spectra of (a) the doubly protonated species and (b) the doubly cesiated species of BI-32169 (blue traces) and its branched-cyclic topoisomer (red traces). The dashed line represents the TIMS profile of both topoisomers in mixture. Schemes highlight the macrolactam rings in green, the loop residues in blue, the plugs in red and the C-terminal tail in orange. The disulfide bonds are represented by black lines. The *R*, *r*, and *Sr* values are given.

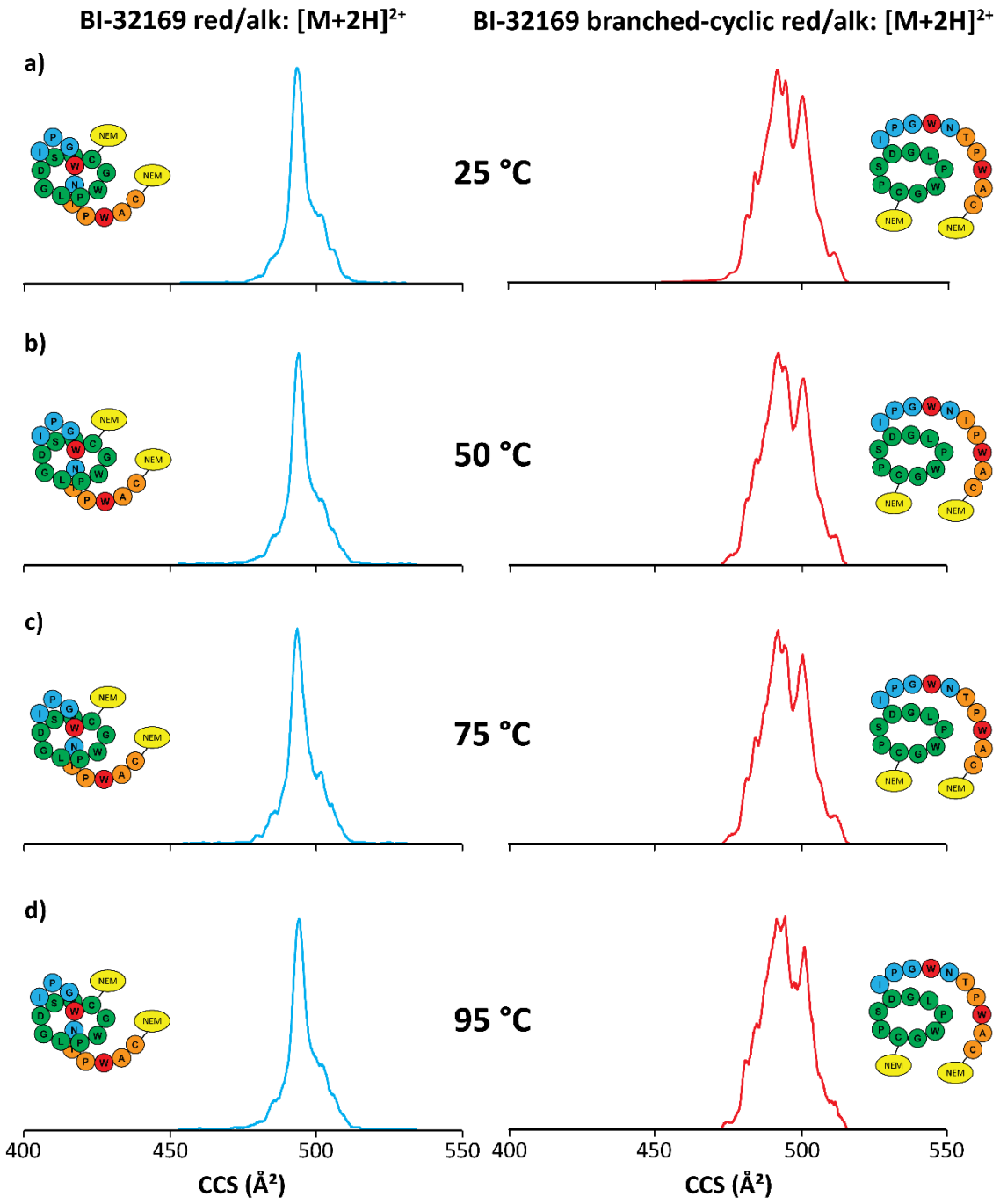

Figure 5. TIMS spectra (*Sr* = 0.3 V/ms) of the doubly protonated species of the reduced/alkylated BI-32169 (blue traces) and the corresponding branched-cyclic peptide (red traces) at (a) 25 °C, (b) 50 °C, (c) 75 °C and (d) 95 °C. Schemes highlight the macrolactam rings in green, the loop in blue, the plugs in red and the C-terminal tail in orange. The alkylating reagents (NEM) are represented in yellow.

GRAPHICAL ABSTRACT